J. For. Res. (2023) 34:677–691
https://doi.org/10.1007/s11676-022-01519-9

ORIGINAL PAPER

Comparative histology, transcriptome, and metabolite profiling unravel the browning mechanisms of calli derived from ginkgo (*Ginkgo biloba* L.)

Xiaoming Yang[1] · Qi Xu[1] · Linlin Le[1] · Tingting Zhou[1] · Wanwen Yu[1] · Guibin Wang[1] · Fang-Fang Fu[1] · Fuliang Cao[1]

Received: 10 January 2022 / Accepted: 6 April 2022 / Published online: 16 August 2022

Abstract *Gingko biloba* accumulates high levels of secondary metabolites of pharmaceutical value. Ginkgo calli develop a typical browning that reduces its regenerative capacity and thus its usefulness. To elucidate the browning mechanism, histological, transcriptomic, and metabolic alterations were compared between green and browning calli derived from immature ginkgo embryos. Histological observations revealed that browning calli had a more loosely arranged cell structure and accumulated more tannins than in green calli. Integrated metabolic and transcriptomic analyses showed that phenylpropanoid metabolism was specifically activated in the browning calli, and 428 differentially expressed genes and 63 differentially abundant metabolites, including 12 flavonoid compounds, were identified in the browning calli compared to the green calli. Moreover, the expression of flavonol synthase (*FLS*) and UDP-glucuronosyl-transferase (*UGT*) genes involved in the flavonoid pathway was more than tenfold higher in browning calli than in green calli, thus promoting biosynthesis of flavonol, which serves as a substrate to form glycosylated flavonoids. Flavonoid glycosides constituted the major coloring component of the browning calli and may act in response to multiple stress conditions to delay cell death caused by browning. Our results revealed the cellular and biochemical changes in browning callus cells that accompanied changes in expression of browning-related genes, providing a scientific basis for improving ginkgo tissue culturability.

Keywords Ginkgo · Callus browning · Histology · Transcriptome · Metabolite · Flavonoid biosynthesis

Introduction

Although plant tissue culture is an extremely valuable tool for producing disease-free plants, propagating and conserving plant germplasm, producing active compounds, and genetically transforming plants (Espinosa-Leal et al. 2018), browning of the callus, is a substantial problem for woody plant tissue cultures. The explants release brown compounds or phenolics as a result of oxidation during dedifferentiation and/or re-differentiation of the tissue (Laukkanen et al. 2000; Phillips and Garda 2019). Tissue-cultured seedlings with severe browning accumulate high levels of phenolic compounds, including phenolic acids, polyphenols, and lignans (Cheynier 2012; Dong et al. 2016; Irshad et al. 2017). In most cases, the quantity of phenolic compounds

Project funding: This work was supported by the Natural Science Foundation of Jiangsu Province (BK20210611), the China Postdoctoral Science Foundation (2018M642261), the Postdoctoral Science Foundation of Jiangsu Province (2018K197C), the Jiangsu Science and Technology Plan Project (BE2021367) and the National Natural Science Foundation of China (31971689).

The online version is available at http://www.springerlink.com.

Corresponding editor: Yanbo Hu

Supplementary Information The online version contains supplementary material available at https://doi.org/10.1007/s11676-022-01519-9.

✉ Fang-Fang Fu
fffu@njfu.edu.cn

✉ Fuliang Cao
fuliangcaonjfu@163.com

[1] Co-Innovation Center for Sustainable Forestry in Southern China, Nanjing Forestry University, Nanjing 210037, People's Republic of China

is proportional to the degree of browning (Altunkaya and Gökmen 2009).

Multiple oxidases, including peroxidase (POD) and polyphenol oxidase (PPO), cause browning by catalyzing the oxidation of phenols to quinones, which are polymerized to generate brown pigments and produce toxic substances. These substances severely impede micropropagation by inhibiting cell growth and causing cell death (Mustafa et al. 2011; Dong et al. 2016). Phenylalanine can be converted to free phenolic substrates for POD production via the catalytic activity of phenylalanine ammonia-lyase (PAL), which also promotes PPO synthesis and exacerbates callus browning (Shi et al. 2013; Dong et al. 2016). In plant tissue cultures, different levels and combinations of growth regulators or reductants (for example, polyvinylpyrrolidone, ascorbic acid, active carbon, calcium chloride, L-cysteine, and 2-aminoindane-2-phosphonic acid) have been found to reduce browning damage to the calli; however, this strategy is not effective for all plants, particularly those that brown easily (Singh 2018; Phillips and Garda 2019). Furthermore, various adsorbents and antioxidants have also been used in culture media to mitigate tissue browning, but they may have a negative effect on callus induction, somatic embryogenesis, and *Agrobacterium*-mediated transformation (Kwak and Lim 2005; Dong et al. 2016). In plant cell cultures, various hormones and concentrations also substantially affect browning (Tang et al. 2004; Suekawa et al. 2019). Browning hinders the application of tissue culture to many plants. Controlling the activation of specific genes or metabolites linked to callus browning may therefore be an effective strategy to combat explant browning.

Ginkgo (*Ginkgo biloba* L.; Ginkgoaceae) is considered a "living fossil", as it is an ancient dioecious gymnosperm that dates from the Jurassic period (Zhou 2009). Ginkgo has been utilized as a valuable medicinal tree for thousands of years, according to the *Compendium of Materia Medica*, a renowned medical book from the Ming Dynasty in China (AD. 1368–1644) (Yang et al. 2021a). Gingko leaves and nuts contain several pharmacological components, such as flavonoids and terpene lactones, which are widely used to treat and protect against many illnesses (for example, lowering blood pressure and exhibiting antioxidant, anti-inflammatory, and anti-tumour activities) in healthcare systems around the world (Nash and Shah 2015; Eisvand et al. 2020; Zhang et al. 2021). Ginkgo is also considered an important economic and ecotype tree species as it accumulates high levels of secondary metabolites, has ornamental value, and is highly resistant to biotic and abiotic stresses (Wang et al. 2020). When cultivated under natural conditions, the pharmaceutical components of ginkgo are relatively low as they are impeded by habitat and season. Thus, in vitro tissue culture and regeneration of ginkgo from various explants could be an effective method to enhance its production of pharmaceutical compounds (Hao et al. 2009; Popova et al. 2009; Cheng et al. 2014). However, browning is a recalcitrant problem for in vitro ginkgo cultures, resulting in poor explant development, tissue culture failure, and detrimental effects on ginkgo regeneration (Radia and Jocelyne 2003). Remarkably, the browning gingko callus produces large amounts of the monophenolic compound salicylic acid (Phongtongpasuk and Piemthongkham 2014). Various oxidase inhibitors and antioxidants were added to the ginkgo tissue culture growth media; however, they did not have conclusive ameliorative effect on ginkgo calli browning, which limited the commercial synthesis of flavonoids and terpene lactones via tissue cultures. The development of transgenic plants is primarily based on the efficiency of in vitro regeneration systems; therefore, in vitro culture of ginkgo may be an effective alternative method for cultivating ginkgo plants with desirable metabolites or agronomic traits. However, callus browning remains a major obstacle in the development of a high-efficiency ginkgo tissue culture system.

Morphological differences between browning and green calli have been detected in different species, and an improved understanding of these differences would contribute to the development of effective in vitro culture systems (Laukkanen et al. 2000; He et al. 2009; Kaewubon et al. 2015). High-throughput transcriptome sequencing with high efficiency in discovering differentially expressed genes (DEGs) has been successfully used to identify genes that are potentially associated with the browning characteristics of the calli (Gao et al. 2020; Zhang et al. 2020). Several enzymatic browning-related DEGs, such as *PPO*, *PAL*, *POD*, catalase (*CAT*), and superoxide dismutase (*SOD*), have been consistently identified using transcriptome analysis (Xu et al. 2015a, b; Gao et al. 2020). Metabolomic analysis is also crucial for understanding systematic biology by enabling all metabolites in an organism to be quantified (Alseekh and Fernie 2018). Furthermore, the combination of transcriptome and metabolome studies has helped reveal many functional genes and elucidate complicated metabolic pathways (Fang and Luo 2019). However, the changes in the histological characteristics and gene expression and metabolite abundance that occur during the callus browning process in ginkgo have not yet been fully elucidated. In the present study, by conducting comparative histology, transcriptomic, and metabolomic analyses, we learned more about the mechanism of browning in calli derived from immature embryos of ginkgo. These results provided a theoretical foundation for the development of an effective strategy to reduce browning in ginkgo tissue cultures.

Materials and methods

Plant materials and callus induction

Immature seeds (nearly 170 days after pollination) of ginkgo 'Dafozhi' were collected from the ginkgo germplasm resource nursery of Nanjing Forestry University, Nanjing, China, on the 20 August 2019. The surfaces of the seeds were sterilized in 70% (v/v) ethanol for 1 min and 3% (v/v) sodium hypochlorite solution for 15 min. After disinfestation, the seeds were rinsed in excess of five times with sterile distilled water. Immature embryos (~ 2 mm) extracted from sterilized seeds were wounded and then used to induce callus formation in Douglas-fir cotyledon revised (DCR) basal medium supplemented with 20 g/L sucrose, 0.5 g/L casein hydrolysate, 0.45 g/L glutamine, 2.5 g/L phytagel, 2 mg/L 2,4-dichlorophenoxyacetic acid, 0.5 mg/L 6-benzylaminopurine, 0.5 mg/L kinetin, and 10 mg/L citric acid. The pH of all culture media was adjusted to 5.4 before autoclaving at 120 °C for 20 min.

To induce callus proliferation, we incubated the immature embryos used as explants were incubated in culture medium in a chamber in the dark at 25 ± 1 °C for 4 weeks, then with a 12-h photoperiod (90 μmol m^{-2} s^{-1}). Subsequently, the induced calli were collected after 21 (green calli) and 35 (browning calli) days. A total of 15 plates were used with five explants per plate. Three biological replicates of each sample were immediately preserved in liquid nitrogen and then stored at − 80 °C freezer for subsequent transcriptome and metabolism analyses.

Histological, histochemical, and scanning electron microscopy analyses

Different pieces of calli were fixed in formaldehyde–acetic acid–alcohol (FAA; formaldehyde: glacial acetic acid: 70% ethanol; 5:5:90 v/v/v) at the end of each culture period. Fixed tissues were dehydrated in aqueous solutions of tertiary butyl alcohol and cut into 6-μm thick sections using a rotary microtome. To identify the presence of carbohydrates and cell walls, periodic acid-Schiff (PAS) reagent to detect polysaccharides and the differential stain toluidine blue O were used to visualize meristematic cells. All sections were viewed with a Leica DM500 light microscope (40 × /0.65 NA/0.31 mm W.D., Leica, Germany) and imaged using a Leica ICC50W digital camera (Aptina 1/2-inch CMOS sensor, pixel size = 3.2 μm × 3.2 μm, pixel resolution = 2048 × 1536).

Differences in cellular structures between the green and browning calli were further investigated using scanning electron microscopy. Small pieces of calli (4 − 6 mm) were collected and fixed with FAA (10% formaldehyde, 5% acetic acid, 45% ethanol). The fixed samples were washed with 0.1 M phosphate buffer and dehydrated through an ethanol series (30%, 50%, 70%, 80%, 90%, 95%, and 100% ethanol). Then, all samples were dried in a critical point dryer and examined with a scanning electron microscope (Hitachi, Tm 30,000, Tokyo, Japan).

Metabolite extraction and analysis using UPLC-Q-TOF MS

Six samples were collected from green and brown calli for metabolomic analysis and frozen at − 80 °C until used. The frozen tuberous calli were ground into a fine powder, and 50 mg powder was extracted using a 400 μL methanol–water (4:1, v/v) solution with 0.02 mg/mL L-2-chlorophenylalanine as an internal standard. The mixture was precipitated at − 10 °C, then homogenized at 5 °C with a high-throughput tissue crusher (Wonbio-96c, Shanghai Wanbo Biotechnology Co., Ltd, Shanghai, China) at 50 Hz for 6 min and an ultrasound at 40 kHz for 30 min. Samples were then frozen for 30 min at − 20 °C to precipitate proteins. After centrifugation at 4 °C for 15 min, the supernatant was filtered and transferred to new glass tubes for further analysis using an Agilent 1290 series UPLC system. Metabolites in the extraction solution were separated using a Zorbax Eclipse Plus-C18 column (2.1 × 100 mm, 1.8 μm, Agilent) at 35 °C and 0.004% acetic acid as mobile phase A and 0.004% acetic acid in acetonitrile as mobile phase B in positive ion mode. The metabolites were determined by gradient elution as follows: 0–5% B for 0–0.1 min, 5–25% B for 0.1–2 min, 25–100% B for 2–9 min, 100–100% B for 9–13 min, 100–0% B for 13–13.1 min, and 0–0% B for 13.1–16 min. The flow rate was set at 0.4 mL/min, and sample injection volume was 2 μL. An Agilent 6538 Q/TOF mass spectrometer (Agilent, Santa Clara, CA, USA) equipped with an ESI interface was used to separate the components. The optimised ESI parameters were sheath gas flow rate of 40 arb, aux gas flow rate of 10 arb, capillary temperature of 320 °C; full MS resolution of 70,000, MS/MS resolution of 17,500, normalized collision energy of 20–40-60 V rolling for MS/MS, and ion-spray voltage floating of 3.5 kV (positive) and − 2.8 kV(negative).

Metabolite data preprocessing and annotation

Peaks were detected and aligned using Progenesis QI 2.3 (Nonlinear Dynamics/Waters Corp., Milford, MA, USA). A data matrix was generated that contained the retention time (RT), mass-to-charge ratio (m/z) values, and peak intensities from the UPLC-MS analysis. Metabolites were identified by retrieving data from metabolite databases (Smith et al. 2005), MassBank (Horai et al. 2010), MS-DIAL software (Tsugawa et al. 2015), and relevant published literature. Some unidentified structural metabolites were detected based on the characteristic fragments, exact molecular mass,

RT, and neutral losses. The R software (www.r-project.org/) was used to perform principal component analysis (PCA), hierarchical cluster analysis, and supervised multiple regression orthogonal partial least-squares discriminate analysis (OPLS-DA). To evaluate the significance of the metabolites, we performed variable importance in projection (VIP) analysis in the OPLS-DA model, which was dimensionality reduction, thus allowing the initial screening of metabolites that differ between green and brown calli. The VIP value indicates the strength of the effect of the group differences of the corresponding metabolites in the classification discrimination of each group of samples in the model. It could also be combined with *P*-values or fold changes in a univariate analysis for further screening for differential metabolites. Pairwise comparisons between the two groups were also conducted, and the metabolites in each pair were considered candidate metabolites when there was a significant difference with a VIP ≥ 1, fold change (FC) ≥ 2 or ≤ 0.05, and $P < 0.05$, as determined by Student's *t*-test.

RNA isolation and sequencing analysis

Total RNA from the green and brown calli was extracted using the extraction protocol of the Total RNA Isolation Kit (BioTeke Corp., Beijing, China). High-quality RNA sequencing (RNA-seq) was performed using the Illumina HiSeq-2500 platform, and paired-end reads of up to 150 bp were generated. The Q20, Q30, and GC content of the clean data were calculated to evaluate the sequencing quality. Low-quality sequences and adapters of the raw reads were filtered out using the FastQC software (http://www.bioinformatics.babraham.ac.uk/projects/fastqc/). Then, clean reads were mapped to the ginkgo genome (Zhao et al. 2019) using Hisat2 v2.0.5 (Pertea et al. 2016). StringTie V1.3.3b (Pertea et al. 2016) was used to calculate the average expression of each gene in fragments per kilobase of transcript per million mapped fragments (FPKM). The RNA-seq data set was deposited in the Sequence Read Archive (SRA) database of NCBI (BioProject ID PRJNA753781).

Identification and function analysis of DEGs

DEGs between the green and brown calli were calculated with the DESeq R package (1.18.0) with adjusted *P*-values. DEGs were selected with an adjusted *P*-value < 0.05 and |log2 FC| ≥ 1. A similarity search using BLAST with an E-value cut-off of $1e-5$ was carried out against publicly available nucleotide and protein databases, including the non-redundant protein database (NR), Cluster of Orthologous Groups of Protein (COG), Swiss-Port, Pfam. The go-seq R package (Young et al. 2010) was used for Gene Ontology (GO) functional enrichment and the KO-based annotation system (KOBAS) (Xie et al. 2011) for the Kyoto Encyclopedia of Genes and Genomes (KEGG) pathway analyses of the DEGs.

Quantitative real-time PCR (qRT-PCR) analysis

Genes in the phenylpropanoid and flavonoid biosynthesis pathways were quantified using qRT-PCR analysis as previously described (Zhou et al. 2020) in a 20-μL reaction volume using the SYBR Premix Ex Taq Kit (TaKaRa) and an Applied Biosystems thermal cycler (Foster City, CA, USA). *GbGAPDH* (MN535380) was selected as the reference gene (Zhou et al. 2020). The reaction conditions were 95 °C for 30 s, 40 cycles of 95 °C for 5 s, and 60 °C for 30 s. Relative expression levels were calculated using the $2^{-\Delta\Delta Ct}$ method (Livak et al. 2001). qRT-PCR analysis was performed with three biological replicates, and the primer sequences were listed in Table S1.

Integrative analysis of metabolome and transcriptome

Based on the DEGs and differentially abundant metabolites (DAMs), an integrative analysis of the gene expression and metabolite content was conducted using the Pearson correlation with the R software (http://R-cran.org), and only associations with a *P*-value ≤ 0.05 were retained. The relationships between the DEGs and DAMs were visualized using R (http://R-cran.org) and Cytoscape (http://cytoscape.org/) software.

Results

Differences in the morphological, histological, and histochemical features of the green and browning calli of ginkgo

Immature ginkgo embryos formed callus and were cultured on modified DRC medium. The calli became discolored during their development from the green to the browning stages (Fig. 1a and b). Small brown spots first occurred on the surfaces of the callus masses after 5 weeks and turned dark brown after nearly 7 weeks. The cells of the green and browning calli obviously differed in appearance and size when analyzed with scanning electron microscopy. Histological analysis demonstrated that the majority of the cells in the browning calli were loose and irregular (Fig. 1d), while those of the green calli consisted of homogeneous, tightly arranged parenchyma cells (Fig. 1c). The two callus types also differed in the accumulation of insoluble carbohydrates (PAS reaction) and ergastic substances including tannins (toluidine blue [TBO] staining). The green calli accumulated more insoluble carbohydrates (starch) than in the browning calli (Fig. 1e and f), and TBO stained the browning calli a

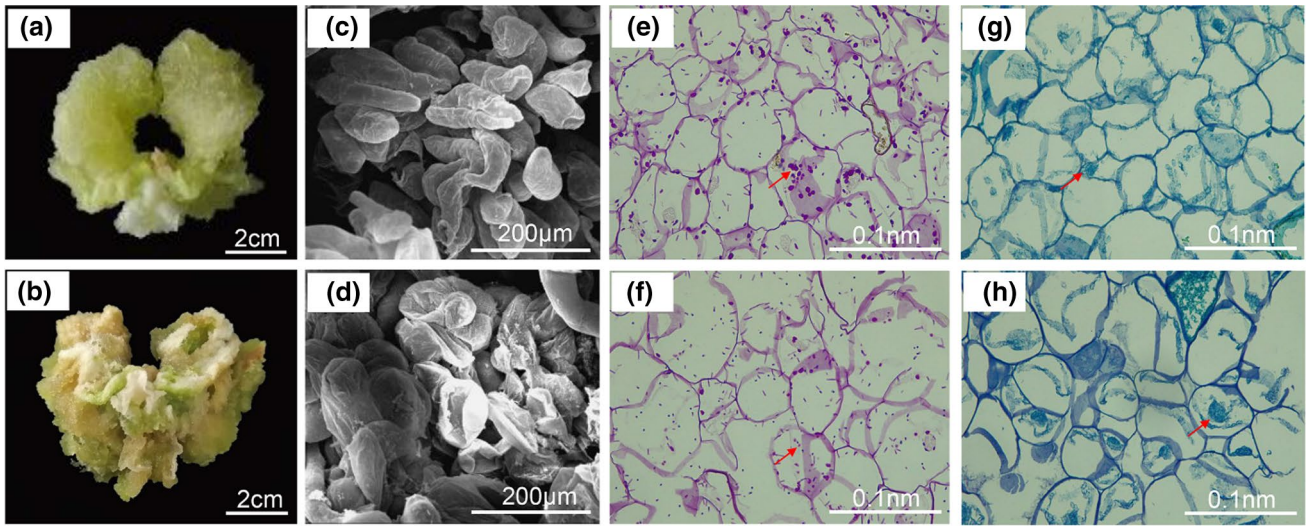

Fig. 1 Morphological and biochemical characteristics of green and browning calli derived from immature ginkgo embryos. Callus induction in ginkgo: green color appears after 3 weeks (**a**) and browning after 5 weeks (**b**). Green calli show uniform and tightly arranged parenchyma cells (**c**), in contrast to the browning calli with variable and disorganized cells with partially collapsed cells (**d**). After PAS staining, green callus had more insoluble carbohydrates (red arrow, e) than in the browning callus (red arrow, **f**). A slight green color after toluidine blue O (TOB) staining indicates an absence or a low level of tannin in green callus (**a** red arrow, **g**), whereas the dark green color of browning callus indicates a high amount of tannin (**a** red arrow, **h**)

dark green in almost all regions of the cells, indicating more tannins than in the green calli, which stained green in only a few parts of the cells (Fig. 1g and h).

Metabolites in the green and browning calli

To obtain a more comprehensive and accurate understanding of the different metabolites in the green and browning ginkgo calli (Gb_GC1, Gb_GC2, and Gb_GC3 for the green calli; Gb_GB1, Gb_GB2, and Gb_GB3 for browning calli), an untargeted metabolomics strategy was used to analyze their metabolite profiles. A total of 1252 metabolites, including 567 and 685 in the positive and negative ion modes, respectively, were identified in the calli using LC–MS/MS. Based on the metabolite concentration data, a hierarchical heatmap clustering analysis of the samples was carried out, and three biological replicates were grouped together, which indicated the reliability of the generated metabolome data (Fig. S1). DAMs between the green and browning callus samples clustered into main groups, which contrasting levels of accumulation (Fig. S2). Furthermore, the metabolites from the green and browning calli separated into different groups in the PCA (Fig. 2a). Notably different metabolites between the green and browning calli were revealed using PLS-DA (Fig. 2b) and OPLS-DA (Fig. 2c), which showed a clear separation between the two types of calli. As shown in Fig. 2d, the 200-response sorting tests of the OPLSA-DA model further proved the reliability of our data as the model with the best fit at the slope of the Q2Y, and R2Y lines were far away from the horizontal line, and Q2 was greater than zero for the response permutation testing. Coincidently, PLS-DA and OPLS-DA results were consistent with those of PCA. In general, we denoted metabolites with VIP > 1 as being involved in group discrimination. Therefore, FC (≥ 2 or ≤ 0.05) and VIP (≤ 1) values were simultaneously considered when screening metabolites that differed significantly between the green and browning callus samples (Fig. 3, top 30 metabolites). A total of 63 metabolites (11 downregulated and 52 upregulated) were significantly different (Table S2). All flavonoids (15 metabolites, 28.85%) were found to be upregulated among these DAMs. KEGG classification and enrichment analyses showed that DAMs were mainly involved in the phenylpropanoid metabolism, phenylalanine, tyrosine and tryptophan biosynthesis pathways (Fig. 4).

Assembly and annotation of the green and browning calli

Based on three biological replicates, the transcriptome sequencing of the six samples yielded 43.95 Gb of clean data, with an average of 7.33 Gb for each sample with 92.99 of the bases scoring Q30 or above (Table S3). After assembly, 65,096 unigenes were generated, and 37,823 of these exceeded 1 kb. The average mapping rate reached 94.55%, indicating that the data obtained were reliable for further profile studies on gene expression. Multiple databases, including the NR, COG, Swiss-Port, KEGG, GO and Pfam

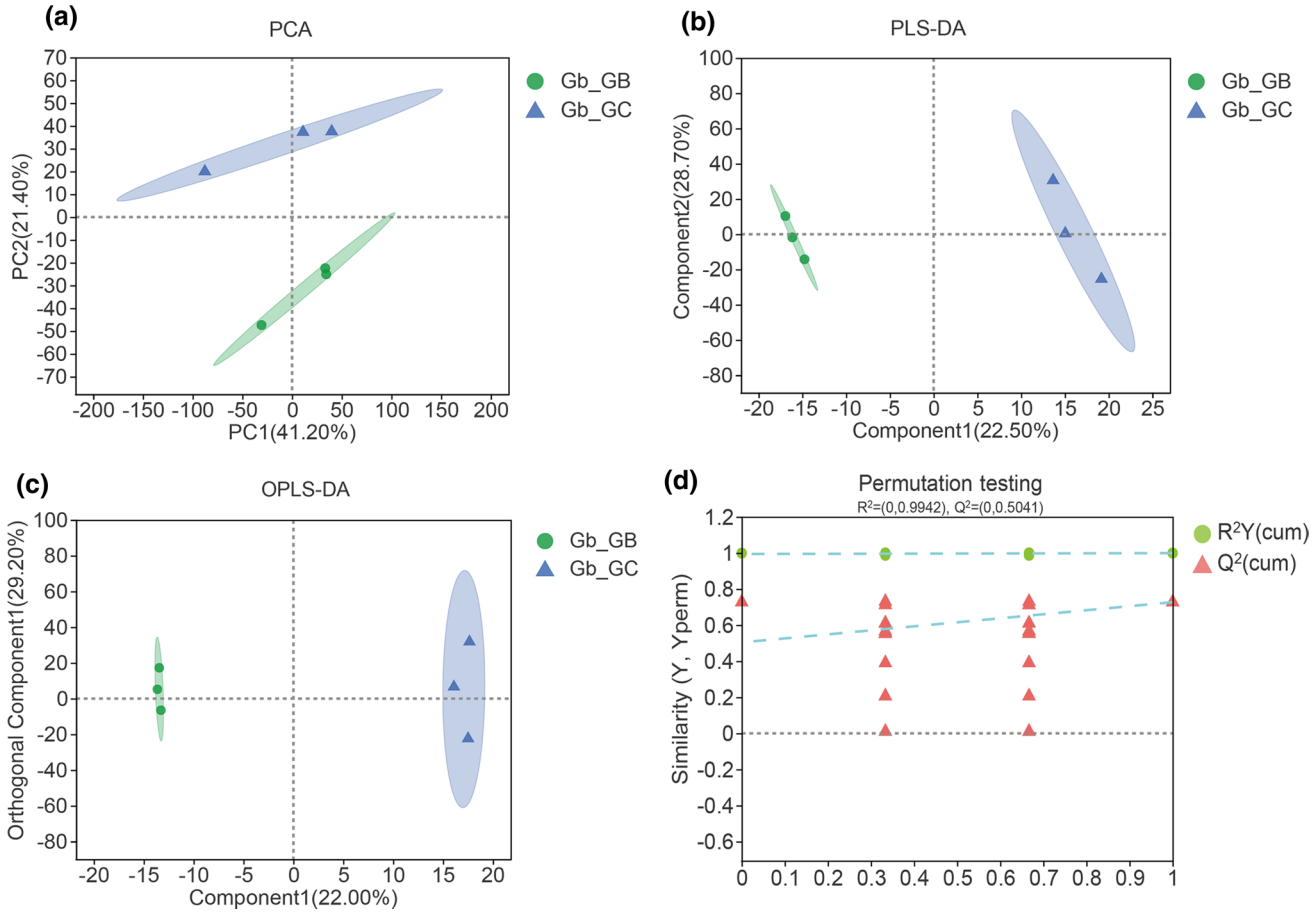

Fig. 2 Metabolomic profiling of green (Gb_GC) and browning (Gb_GB) calli from ginkgo. Plots of PCA (**a**), PLS-DA (**b**), and OPLS-DA (**c**) for the comparison groups; scores for the analysis of the metabolites, and the 200-response sorting tests of the OPLS-DA model (**d**) in the green and browning calli

databases, were used for functional annotations of unigenes, resulting in annotations for 26,783, 24,492, 21,432, 11,294, 22,992, and 18,271 unigenes, respectively (Fig. S3). The unigenes in the NR database accounted for the greatest proportion, accounting for 21.38% of the total.

Functional classification of the DEGs in the green and browning calli

To identify DEGs, we compared the FPKM values of each gene in the green and browning calli. A total of 428 significant DEGs (153 downregulated and 275 upregulated genes) between the green and browning callus libraries were detected. The upregulated and downregulated genes between the green and browning calli could be distinguished using the high correlation coefficients after comparison of the different gene expression profiles in the heat map (Fig. S4) and the volcano plot (Fig. 5a). The similar color of the DEGs indicates that all transcriptome samples had a significant correlation coefficient.

The differentially expressed unigenes were then functionally categorized using KEGG (Fig. 5b) and GO analyses (Fig. S5). The GO classification yielded three GO categories: cellular component (CC), biological process (BP), and molecular function (MF); 20 GO terms were obtained within these categories. For the CC category, unigenes were matched with seven GO terms wherein membrane part was the largest subcategory. Within the MF category, binding and catalytic activity were the most abundant subcategories containing five GO terms. For the BP category, unigenes were matched to eight GO terms, and the largest subcategory was cellular process. The KEGG annotation system was used to determine the synthetic pathways of the bioactive components by mapping the assembled unigenes, and many more unigenes were in the pathways metabolism (166 unigenes), environmental information processing (20 unigenes), and organismal systems (12 unigenes). These data represented the overall functions of the DEGs between the green and browning calli and

Fig. 3 Expression profiles of the differentially abundant metabolites (top 30), and the VIP (variable importance in projection) value of each metabolite obtained from the OPLS-DA with a threshold of 1.0

improved our understanding of the differences between the two states of calli at the gene function level.

In the KEGG enrichment analyses, 123 metabolic pathways were associated with the DEGs in the two states of ginkgo calli (Fig. 5b). Of these, the most significantly enriched pathways (the top 20 KEGG pathway, $P < 0.05$) based on the upregulated and downregulated DEGs were phenylpropanoid biosynthesis; cutin, suberin, and wax biosynthesis; flavonoid biosynthesis; and fatty acid biosynthesis. The enrichment of the KEGG pathways identified significant DEGs between the two different types of calli, indicating that these pathways might play a vital role in callus browning.

To explore possible divergent expression patterns between the green and browning calli, we also selected several flavonoid pathway-related genes in ginkgo that are homologues to the ones involved in other plants based on functional annotations: phenylalanine (*PLA*), cinnamate-4-hydroxylase (*C4H*), 4-coumaryl coenzyme A (*4CL*), chalcone synthase (*CHS*), chalcone isomerase (*CHI*), flavanone 3-hydroxylase (*F3H*), flavonoid 3′-hydroxylase (*F3'H*), flavonol synthase (*FLS*), dihydroflavonol 4-reductase (*DFR*), anthocyanidin synthase (*ANS*), and anthocyanidin reductase (*ANR*). Based on the enriched KEGG pathways and gene functional annotation, DEG-encoded enzymes involved in flavonoid biosynthesis were identified. Thirty-seven transcripts were differentially affected in the flavonoid pathway; 11 were downregulated, and 26 were upregulated (Fig. 6a). The expression of different transcripts encoding *PAL*, *4CL* and *FLS* was consistently higher in the browning calli than in the green. However, some *C4H*, *CHS*, *F3'H*, *DFR*, and *ANS* homologues showed contrasting expression patterns, indicating that the biosynthesis of flavonoid metabolism components was complex and that multigene families differentially controlled flavonoid biosynthesis in ginkgo. Furthermore, DEGs from the UDP-glycosyltransferase (*UGT*) genes were also identified as they were found to be associated

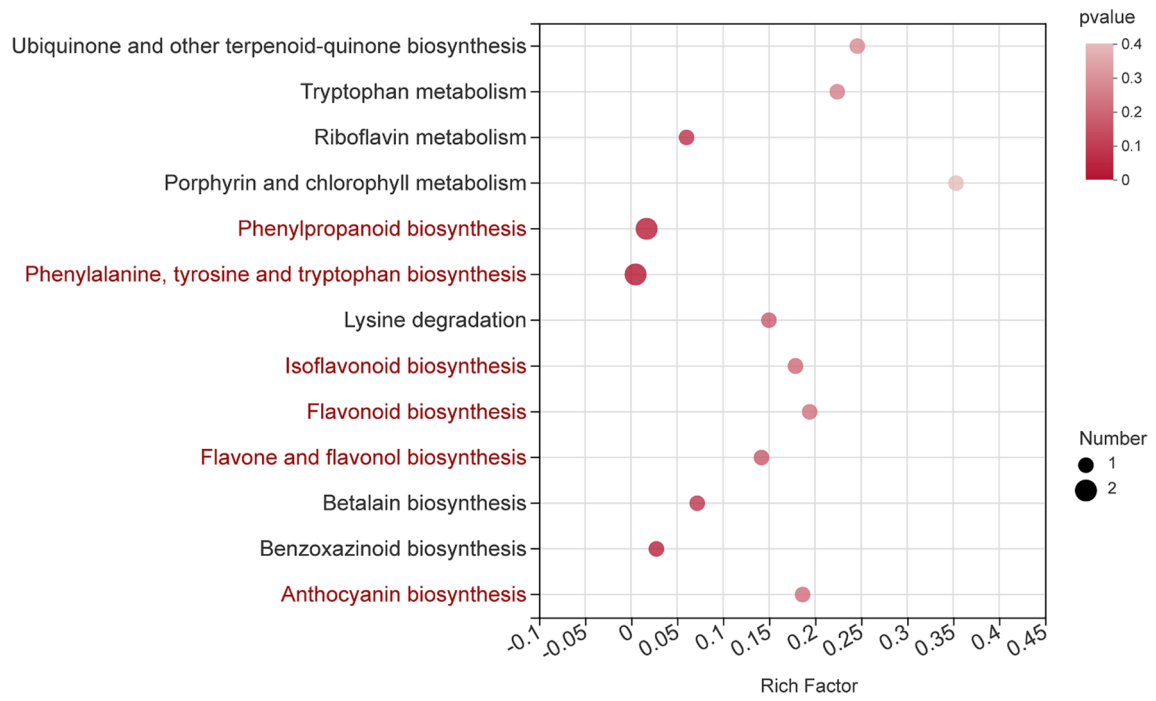

Fig. 4 Scatterplot of the significantly enriched metabolites in the KEGG pathways between the green and browning calli of ginkgo. The *x*-axis and *y*-axis represent the enrichment factor and the pathway name, respectively

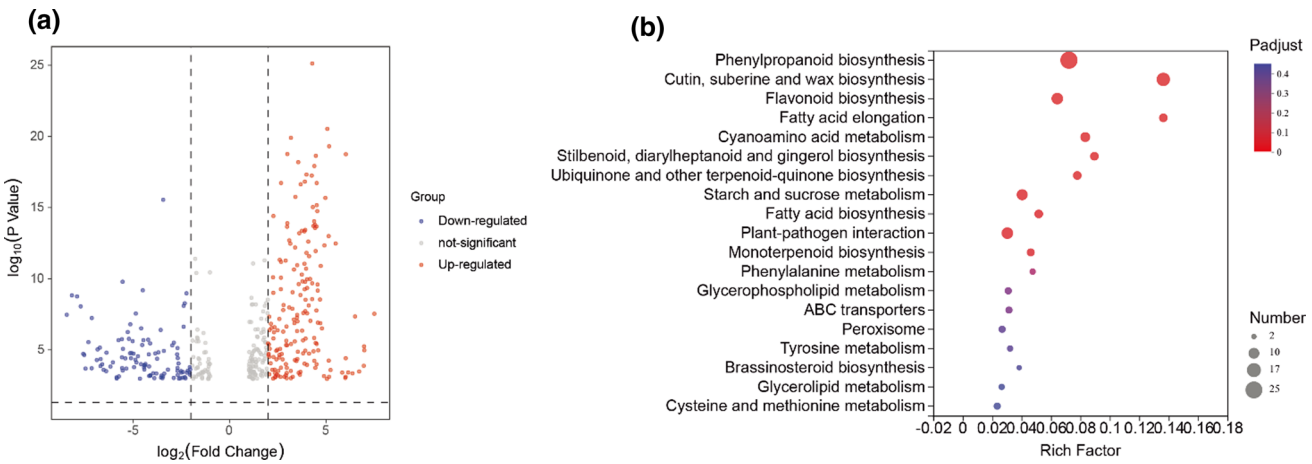

Fig. 5 Differentially expressed genes in the green and browning calli of ginkgo. Volcano plots display the upregulated, downregulated, and unregulated genes (**a**), and the top 20 KEGG terms contributed by the differentially expressed genes (**b**).

with flavonoid glucoside biosynthesis (Fig. 6b). Five *UGTs* were identified, of which three were downregulated and two upregulated in the green calli compared to the browning calli. Strikingly, gene (Gb_34095) expression was more than tenfold higher in the browning calli than in the green calli. This gene has been functionally characterized as involved in the biosynthesis of flavonoid glucosides in ginkgo (Su et al. 2017). To validate the accuracy of the gene expression analysis in this study, 11 transcripts with potential roles in flavonoid biosynthesis were analyzed by qRT-PCR, which showed similar expression patterns to those derived from the transcriptome data (Fig. 6c).

Phenolic alterations between the green and browning calli

The expression heat map of the key metabolites and transcripts for flavonoid synthesis are shown in Fig. S6. The correlation analysis based on the Pearson correlation coefficients for transcriptomic and metabolomic data showed

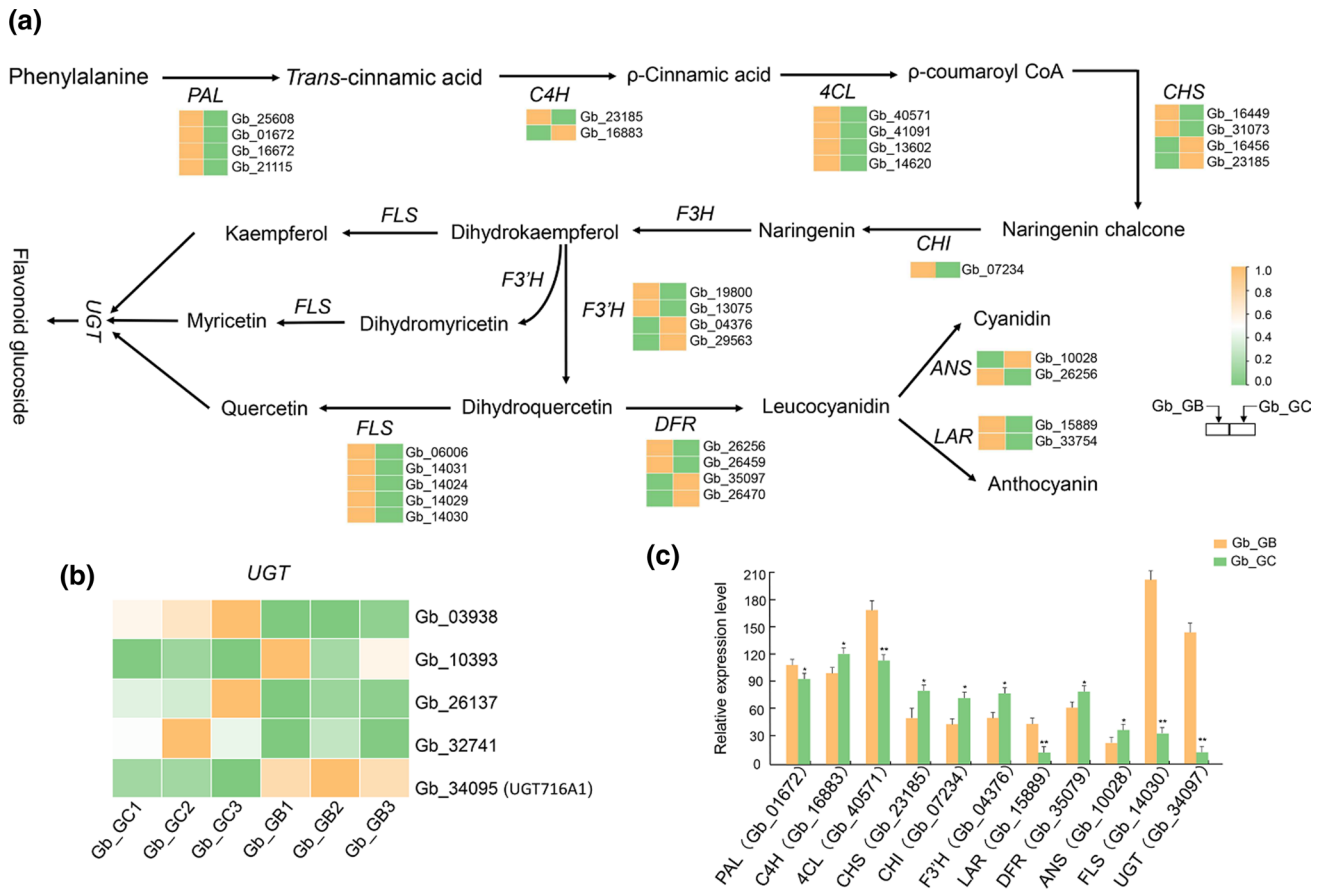

Fig. 6 Biosynthetic pathway of flavonoids in ginkgo. Heat map of the changes in structural genes expressions related to flavonoid metabolism (**a**), including the UDP-glycosyltransferase (*UGT*) gene (**b**). Rectangles marked with orange and green backgrounds represent increased and reduced gene expression, respectively. qRT-PCR results show the expression levels of the 11 flavonoid-related DEGs in the green and browning calli (**c**)

a high correlation between the gene expression and the response strength of the metabolites according to the correlation matrix of the top 30 DEGs and DAMs. The results showed that the phenylpropanoid biosynthetic pathway had a high number of DEGs (4 genes, 13%) and DAMs (12 metabolites, 40%; Fig. S7 and Fig. 7). Twelve different flavonoids were identified in the green and browning calli, with differences not only in quantity but also in type (Fig. S8). Coincidentally, these flavonoids were upregulated when the callus changed from green to browning. Seven metabolites (awobanin, kaempferol 2G-coumaroylrutinoside, petunidin 3-glucoside, genistin, syringetin 3-glucoside, spinacetin, and laricitrin 3-galactoside) were identified from the flavonoid biosynthesis pathway, which had highly positive correlations with at least one gene (correlation coefficients > 0.80). Interestingly, 11 DEGs were positively correlated with syringetin 3-glucoside and spinacetin (correlation coefficient > 0.80), indicating one flavonol synthase gene (*GbFLS*, Gb_14030) and another gene (Gb_28539) that, according to the gene functional annotation, was also associated with phenylpropanoid biosynthesis. Our results identified the gene (Gb_05303) with the highest correlation with quercitrin (correlation coefficient = 0.95); its gene functional annotation was a jacalin-related lectin that plays a vital role in defence signaling and the regulation of growth, development, and response to abiotic stress (Jung et al. 2019). Furthermore, two types of organic acids and their derivatives (6-oxopiperidine-2-carboxylic acid and inositol cyclic phosphate) were found to have a significantly positively correlated with two genes (Gb_05303 and Gb_33606; correlation coefficient > 0.80). While the results demonstrated that many genes were significantly correlated with the majority of the differential metabolites, identifying their functions required further investigation.

Effects of transcription factors on metabolite accumulation in the green and browning calli

Transcription factors are important regulatory factors that interact with genes by specifically binding to *cis*-acting

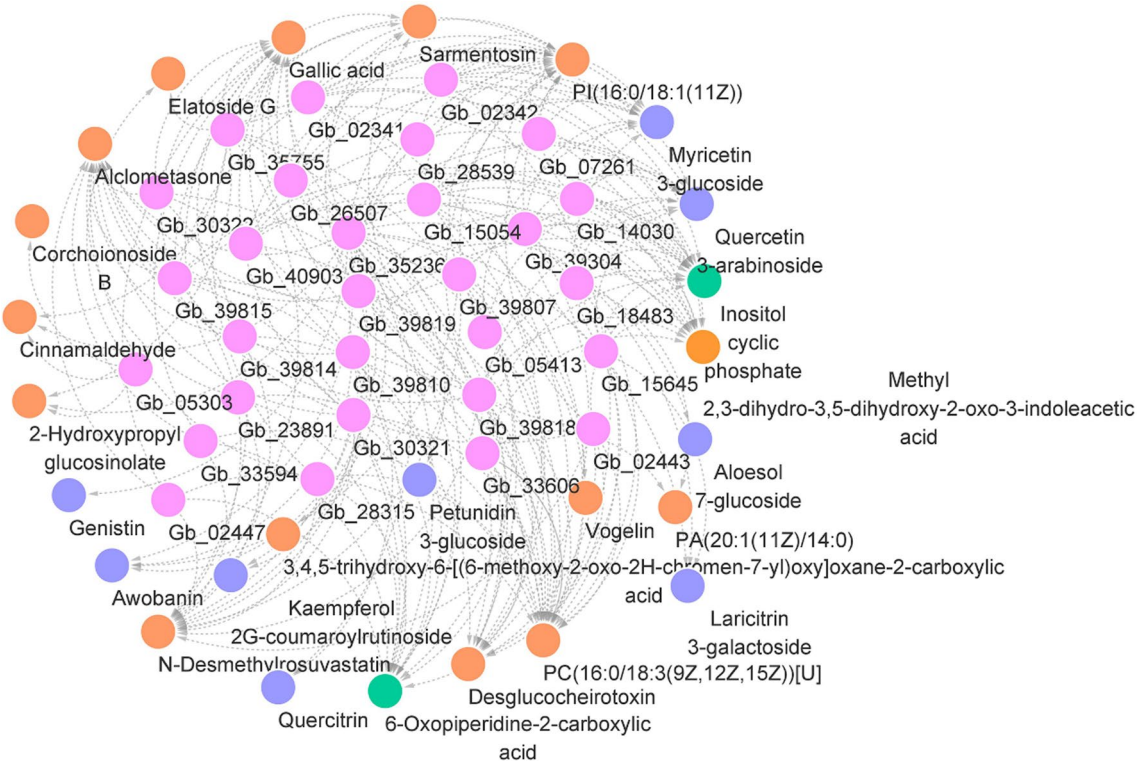

Fig. 7 Correlation analysis of DEGs (top 30) and DAMs (top 30). The pink, purple, green, and orange solid circles indicate the differential expression of genes, flavonoid compounds, organic acids, and other metabolites, respectively

elements to inhibit or activate their expression. Many transcription factors, especially MYBs and basic helix-loop-helix (bHLHs), play a significant role in the synthesis of flavonoids in plants (Xu et al. 2015a, b). Transcriptome data analysis identified 17 DEGs as transcription factors in the browning calli compared to the green calli; these factors could be divided into 10 transcription factor families (Fig. 8a and b). Among these transcription factors, MYB (23.53%), NAC (17.65%), HD-ZIP (11.76%), and AP2 (11.76%) had more potential to modulate the gene expression of members in each family, followed by C2H2, WRKY, SRS, TCP, HSF, and LBD. Specifically, three MYB (3/4, 75%), three NAC (3/3, 100%), two AP2 (2/2, 100%), and one each of C2H2 (1/1, 100%), SRS (1/1, 100%), HSF (1/1, 100%), and LBD (1/1, 100%) were upregulated. However, the expression of other transcription factors was suppressed in the browning calli compared to the green calli. The differences in the expression of the abovementioned transcription factors may contribute to the differential accumulation of metabolites between the green and browning calli of ginkgo.

Discussion

Browning on the surface of calli is common, especially as vigorous calli begin to degrade. The appearance of browning and loss of green color on the surface of calli is thought to be the result of chlorophyll degeneration or incomplete chlorophyll metabolism (Toivonen and Brummell 2008). In addition, oxidative browning, which is caused by phenolic oxidation and leads to the formation of browning pigments, also contributes to callus browning (Kaewubon et al. 2015; Dong et al. 2016). In this investigation, the ginkgo callus color changed from green to brown after 5 weeks on a suitable medium. Microscopic examination indicated significant alterations in the cellular structures of the calli generated from immature ginkgo embryos. The cells of ginkgo green and browning calli clearly differed in size and appearance. While the green calli had relatively uniform and tightly arranged parenchyma cells, the browning calli had a looser and more disordered cell arrangement. Analogous changes in color and cell structure were also observed in other wood

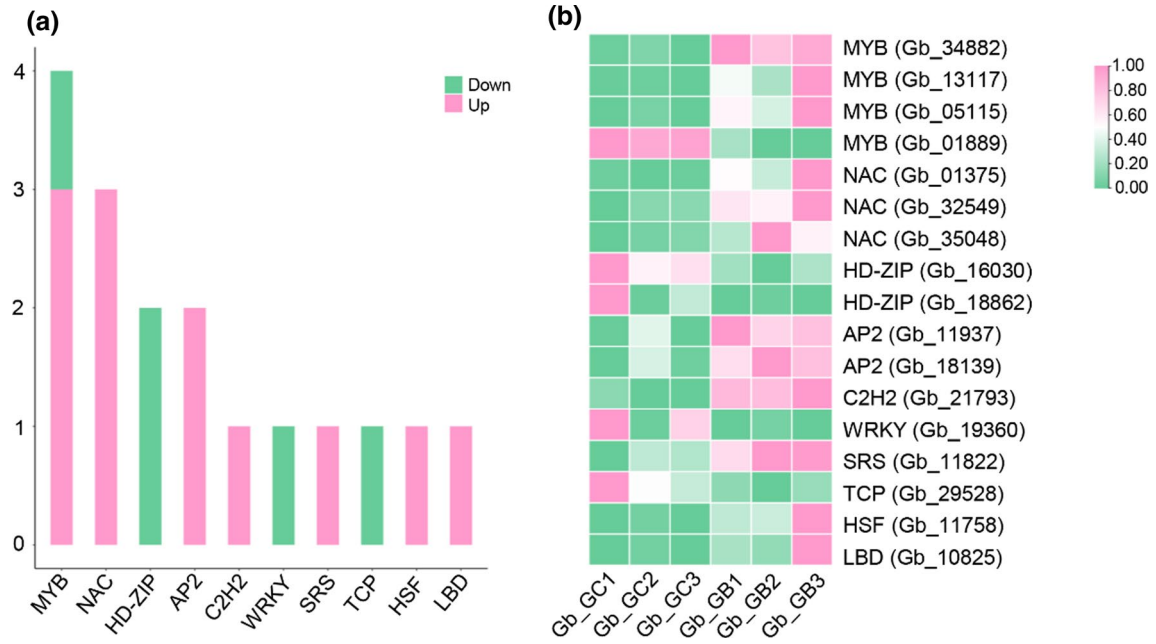

Fig. 8 Transcription factor (TF) categories and their differential expression. The *y*-axis represents the number of TFs, and the *x*-axis represents 10 differentially expressed TF families (**a**). Heatmap showing the expression patterns of different TFs (**b**). Upregulated (pink) and downregulated (green) genes are indicated

plants when browning occurred in their calli. For example, cells of browning calli of *Pinus sylvestris* have a thick cell wall and lack cytoplasm, in direct contrast to its corresponding green calli (Laukkanen et al. 2000). Similarly, spheroid and compactly arranged cells are observed in the non-oxidized calli of *Jatropha curcas*, which is in contrast to cells in browning calli that are irregular and loosely arranged (He et al. 2009). Tannins are typical phenolic compounds and their high accumulation in cells has an adverse physiological effect on cell development, resulting in the destruction of cell membrane integrity and cell death (Santiago et al. 2000; Kaewubon et al. 2015), which partially explains why more uniform and tightly arranged parenchymatous cells were present in the green calli than in the browning calli, and they had lower accumulation of tannins. In addition, in browning calli, multiple different phenolic compounds occupied a large proportion of these upregulated metabolites, which resulted in a dark green color after TBO staining. Carbohydrates are stored in starch grains and are essential for plant development (Eveland and Jackson 2012). However, the current findings suggest that browning calli accumulate fewer insoluble carbohydrates, which means that they lack the energy resources required for further growth, potentially leading to a loss of totipotency in morphogenically competent cells. Based on the histology that we observed at different stages of ginkgo callus development, we speculate that loosely arranged callus cell structures and high accumulation of tannins instead of carbohydrates are typical characteristics of browning calli.

Phenolic compounds, which are the most common plant secondary metabolites, not only participate in responses to biotic and abiotic stresses, but are also involved in controlling callus browning (Kwak and Lim 2005; Gao et al. 2020). The degree of browning in plants is also positively correlated with the abundance of phenolic compounds (Xu et al. 2015a, b; Gao et al. 2020). However, browning is also suppressed by inhibiting the phenylpropanoid pathway or by reducing polyphenol synthesis (Jones and Saxena 2013). Plants respond to multiple abiotic stresses by accumulating high levels or different kinds of flavonoid compounds (Böttner et al. 2021). Browning, as an atypical abiotic stress response for ginkgo calli, could hinder in vitro manipulation of ginkgo and adversely affect its regeneration frequency, resulting in cell death. To defend against multiple abiotic stresses, such as browning, ginkgo calli tended to accumulate more flavonoids, which is consistent with the results of our transcriptome and metabolome analyses. Our results highlighted that the DEGs between the green and the browning calli are involved in diverse pathways, especially phenylpropanoid biosynthesis, that might cause callus browning in ginkgo. Coincidentally, five genes (*PAL*, *4CL*, *CHI*, *FLS,* and *ANS*) were upregulated in browning calli compared to green calli, and they all promoted flavonoid biosynthesis in the brown calli.

Phenylpropanoid biosynthesis starts with the formation of the aromatic amino acid phenylalanine, and *PAL* catalyzes the conversion of phenylalanine into cinnamic acid. *4CL*, together with *C4H*, catalyzes the conversion of cinnamic acid to ρ-coumaroyl-CoA, which is the precursor for many phenylpropanoid products (Dong and Lin 2021). Thus, higher expression levels of the *PAL* and *4CL* genes in the browning ginkgo calli possibly promoted downstream flavonoid biosynthesis by providing more precursor substances. Genes involved in flavonoid biosynthesis pathways are mainly divided into early (such as *CHS*, *CHI*, *F3H*, *F3'H,* and *FLS*) and late (such as *LAR*, *DFR,* and *ANS*) biosynthetic genes according to their locations in the pathways (Yonekura-Sakakibara et al. 2019; Wen et al. 2020). Three genes (*CHI*, *FLS*, and *LAR*) had higher expression levels in the browning calli than in the green calli. The enzymes encoded by the early biosynthetic genes (*CHI* and *FLS*) would catalyze flavonol biosynthesis, whereas the late biosynthetic gene (*LAR*) would lead to anthocyanin biosynthesis in ginkgo. Flavonoid biosynthesis is predominantly regulated by multiple transcription factors at the transcription level, especially the MYB transcription factors that are conserved in regulating plant flavonoid biosynthesis (Ma and Constabel 2019; Dong and Lin 2021; Yang et al. 2021a).

We comprehensively analyzed the transcriptome profiles of the green and browning calli and found that three members of the MYB transcription factors had higher expression in the browning calli than in the green. In contrast, among these three transcription factors, the one encoded by the gene (Gb_34882) was homologous to *GbMYBFL*, which has been demonstrated to be positively related to flavonoid biosynthesis, and the overexpression of *GbMYBFL* in *Arabidopsis* is sufficient to induce flavonoid and anthocyanin accumulation (Zhang et al. 2018; Yang et al. 2021b). In other words, the inhibition of the gene (Gb_34882) may contribute to changes in callus color from green to brown in ginkgo. Taken together, our transcriptome sequencing analysis has been successful in identifying candidate functional genes involved in ginkgo callus browning and has provided valuable gene resources for better understanding the molecular mechanisms controlling this process. The inhibition of genes related to phenylpropanoid biosynthesis or related transcription factors in ginkgo could be an effective approach to reduce oxidative browning in ginkgo tissue cultures.

The different gene expression profiles in flavonoid biosynthesis were further verified using metabolomic data. Our results showed that the browning calli had higher levels of flavonoid compounds that were major coloring components than in the green calli. Among the flavonoid compounds that differed between the two types of calli, flavonoid glycosides were the most prevalent in the browning calli. Glycosylated flavonoids are multifunctional polyphenolic chemicals found in virtually all higher plant species, and they play crucial roles in plant defence mechanisms against biotic and abiotic stresses (Yonekura-Sakakibara and Hanada 2011; Le Roy et al. 2016; Wilson and Tian 2019). Glycosylation is usually catalyzed by glycosyltransferases (UDP-dependent glycosyltransferases, UGTs) and is essential in regulating the stability, availability, and biological activity of flavonoids (Peng et al. 2017; Su et al. 2017). The majority of *UGT* genes, which are highly inducible by both abiotic and biotic stress factors, are regiospecific rather than substrate-specific, providing plants with a degree of flexibility and allowing them to adjust to changing environmental conditions or evolutionary tendencies (Yang et al. 2018; Dong et al. 2020). Anthocyanin glycosylation has been shown to have a key role in the solubility and stability of these pigments in a variety of flowers (Le Roy et al. 2016). Glycosyltransferase genes can enhance abiotic stress tolerance through increased antioxidant capacity and the upregulated expression of tolerance-related genes in *Arabidopsis* (Li et al. 2018), while UDP-glucosyltransferase regulates metabolic flux redirection to improve abiotic stress tolerance in rice (*Oryza sativa*) (Peng et al. 2017). Collectively, considering the effect of flavonoid glycosides on stress responses, recent studies have suggested that increased levels of flavonoid glycosides may represent a strategy for stabilizing and extending life in plants under multiple stress conditions. In ginkgo, flavonoids are presented in glycosylated forms, indicating the important roles of *UGT* genes in flavonoid metabolism. Coincidentally, according to the gene functional annotation, we identified five members of the *UGT* family with different gene expression levels between the green and browning calli of ginkgo, which highlighted their complicated roles in the biosynthesis of flavonoid glycosides. Furthermore, we found that the gene (Gb_34095) was previously published as *GbUGT716A1*, according to the sequence similarity in ginkgo, and it was activated using a wide range of flavonoid or phenylpropanoid substrates (Su et al. 2017). Overexpression of *GbUGT716A1* in *Arabidopsis* leads to an increase in the accumulation of several flavonol glucosides. In addition, the enzyme encoded by *GbUGT716A1* can synthesize a wide spectrum of flavonoid glycosides, including flavonols, flavones, isoflavones, and flavanol glycosides (Su et al. 2017). Similar to our previous findings, we inferred that the gene (Gb_34095) plays a significant role in the biosynthesis of these glycoside compounds because it had a higher expression level and isoflavonoid *O*-glycoside and flavonoid glycosides in the browning calli were higher than in the green calli. Flavonoid glycoside compounds in ginkgo have also been recognized as one of the three key defence systems in response to herbivore attack (Mohanta et al. 2012). Recent research has also demonstrated that the flavonol glycoside content increases significantly when ginkgo seedlings are under salt stress (Xu et al. 2020). Therefore, we speculated that the higher accumulation of flavonoids glycosides in

ginkgo calli was an effective response to multiple stresses to delay cell death caused by browning. Except for the phenolic compounds, there were other elements responsible for callus browning during phenolic oxidation, such as the action and presence of reactive oxygen species (ROS) and oxidative enzymes (Hesami et al. 2020). Wounding in the explant preparation step, plasmalemma disintegration, breakage of the nuclear envelope, and chloroplast deformation can all result in the accumulation of ROS. Excessive accumulation of ROS accompanies oxidative damage, which leads to callus browning (Gill and Tuteja 2010). Enough transcriptome and metabolite data obtained from more periods of calli development will help us further explore the browning mechanism in ginkgo calli.

Conclusions

To our knowledge, this is the first study to integrate histology, transcriptomic, and metabolomic analyses toward understanding the browning mechanisms of ginkgo callus. Browning calli of ginkgo had loosely arranged cells and accumulated high levels of tannins rather than carbohydrates compared with the green calli. Higher expression of genes associated with the phenylpropanoid pathway was found in browning calli rather than the green calli, resulting in a large quantity of secondary metabolites, particularly the preferential accumulation of flavonoid glucoside compounds that have a wide spectrum of biological activities and are regarded as an efficient defense against the stress and damage caused by callus browning. Therefore, the knowledge gained from our research may hold implications with respect to inhibiting and eliminating browning damage in tissue cultures by modulating the expression of key genes or metabolites, which can promote cellular and metabolic engineering processes and breeding strategies for ginkgo in the future.

References

Alseekh S, Fernie AR (2018) Metabolomics 20 years on: what have we learned and what hurdles remain? Plant J 94:933–942

Altunkaya A, Gökmen V (2009) Effect of various anti-browning agents on phenolic compounds profile of fresh lettuce (*L. sativa*). Food Chem 117:122–126

Böttner L, Grabe V, Gablenz S, Böhme N, Appenroth KJ, Gershenzon J, Huber M (2021) Differential localization of flavonoid glucosides in an aquatic plant implicates different functions under abiotic stress. Plant Cell Environ 44:900–914

Cheng SY, Zhang WW, Sun NN, Xu F, Li LL, Liao YL, Cheng H (2014) Production of flavonoids and terpene lactones from optimized *Ginkgo biloba* tissue culture. Not Bot Horti Agrobo 42:88–93

Cheynier V (2012) Phenolic compounds: from plants to foods. Phytochem Rev 11:153–177

Dong NQ, Lin HX (2021) Contribution of phenylpropanoid metabolism to plant development and plant-environment interactions. J Integr Plant Biol 63:180–209

Dong YS, Fu CH, Su P, Xu XP, Yuan J, Wang S, Zhang M, Zhao CF, Yu LJ (2016) Mechanisms and effective control of physiological browning phenomena in plant cell cultures. Physiol Plantarum 156:13–28

Dong NQ, Sun YW, Guo T, Shi CL, Zhang YM, Kan Y, Xiang YH, Zhang H, Yang YB, Li YC, Zhao HY, Yu HX, Lu ZQ, Wang Y, Ye WW, Shan JX, Lin HX (2020) UDP-glucosyltransferase regulates grain size and abiotic stress tolerance associated with metabolic flux redirection in rice. Nat Commun 11:1–16

Eisvand F, Razavi BM, Hosseinzadeh H (2020) The effects of *Ginkgo biloba* on metabolic syndrome: A review. Phytother Res 34:1798–1811

Espinosa-Leal CA, Puente-Garza CA, García-Lara S (2018) In vitro plant tissue culture: means for production of biological active compounds. Planta 248:1–18

Eveland AL, Jackson DP (2012) Sugars, signalling, and plant development. J Exp Bot 63:3367–3377

Fang CY, Luo J (2019) Metabolic GWAS-based dissection of genetic bases underlying the diversity of plant metabolism. Plant J 97:91–100

Gao J, Xue JQ, Xue YQ, Liu R, Ren XX, Wang SL, Zhang XX (2020) Transcriptome sequencing and identification of key callus browning-related genes from petiole callus of tree peony (*Paeonia suffruticosa* cv. Kao) cultured on media with three browning inhibitors. Plant Physiol Bioch 149:36–49

Gill SS, Tuteja N (2010) Reactive oxygen species and antioxidant machinery in abiotic stress tolerance in crop plants. Plant Physiol Biochem 48:909–930

Hao GP, Du XH, Zhao FX, Shi RJ, Wang JM (2009) Role of nitric oxide in UV-B-induced activation of PAL and stimulation of flavonoid biosynthesis in *Ginkgo biloba* callus. Plant Cell Tiss Org 97:175–185

He Y, Guo XL, Lu R, Niu B, Pasapula V, Hou P, Cai F, Xu Y, Chen F (2009) Changes in morphology and biochemical indices in browning callus derived from *Jatropha curcas* hypocotyls. Plant Cell Tiss Org 98:11–17

Hesami M, Tohidfar M, Alizadeh M, Daneshvar MH (2020) Effects of sodium nitroprusside on callus browning of *Ficus religiosa*: an important medicinal plant. J for Res 31:789–796

Horai H, Arita M, Kanaya S, Nihei Y, Ikeda T, Suwa K, Ojima Y, Tanaka K, Tanaka S, Aoshima K, Oda Y, Kakazu Y, Kusano M, Tohge T, Matsuda F, Sawada Y, Hirai MY, Nakanishi H, Ikeda K, Akimoto N, Maoka T, Takahashi H, Ara T, Sakurai N, Suzuki H, Shibata D, Neumann S, Iida T, Tanaka K, Funatsu K, Matsuura F, Soga T, Taguchi R, Saito K, Nishioka T (2010) MassBank: a public repository for sharing mass spectral data for life sciences. J Mass Spectrom 45:703–714

Irshad M, He BZ, Liu S, Mitra S, Debnath B, Li M, Rizwan HM, Qiu DL (2017) In vitro regeneration of *Abelmoschus esculentus* L. cv. Wufu: Influence of anti-browning additives on phenolic secretion and callus formation frequency in explants. Hortic Environ Biote 58:503–513

Jones AMP, Saxena PK (2013) Inhibition of phenylpropanoid biosynthesis in *Artemisia annua* L.: a novel approach to reduce oxidative browning in plant tissue culture. PloS One 8:e76802.

Jung IJ, Ahn JW, Jung S, Hwang JE, Hong MJ, Choi HI, Kim JB (2019) Overexpression of rice jacalin-related mannose-binding lectin (OsJAC1) enhances resistance to ionizing radiation in *Arabidopsis*. BMC Plant Biol 19:1–16

Kaewubon P, Ilok-Towatana HA, N, Teixeira D, Meesawat U, (2015) Ultrastructural and biochemical alterations during browning of pigeon orchid (*Dendrobium crumenatum* Swartz) callus. Plant Cell Tiss Org 121:53–69

Kwak EJ, Lim SI (2005) Inhibition of browning by antibrowning agents and phenolic acids or cinnamic acid in the glucose–lysine model. J Sci Food Agr 85:1337–1342

Laukkanen H, Rautiainen L, Taulavuori E, Hohtola A (2000) Changes in cellular structures and enzymatic activities during browning of Scots pine callus derived from mature buds. Tree Physiol 20:467–475

Le Roy J, Huss B, Creach A, Hawkins S, Neutelings G (2016) Glycosylation is a major regulator of phenylpropanoid availability and biological activity in plants. Front Plant Sci 7:735

Li Q, Yu HM, Meng XF, Lin JS, Li YJ, Hou BK (2018) Ectopic expression of glycosyltransferase UGT76E11 increases flavonoid accumulation and enhances abiotic stress tolerance in Arabidopsis. Plant Biol 20:10–19

Livak KJ, Schmittgen TD (2001) Analysis of relative gene expression data using real-time quantitative PCR and the $2^{-\Delta\Delta Ct}$ method. Methods 25:402–408

Ma DW, Constabel CP (2019) MYB repressors as regulators of phenylpropanoid metabolism in plants. Trends Plant Sci 24:275–289

Mohanta TK, Occhipinti A, Zebelo SA, Foti M, Fliegmann J, Bossi S, Maffei ME, Bertea CM (2012) *Ginkgo biloba* responds to herbivory by activating early signaling and direct defenses. PLoS ONE 7:e32822

Mustafa NR, de Winter W, van Iren F, Verpoorte R (2011) Initiation, growth and cryopreservation of plant cell suspension cultures. Nat Protoc 6:715–742

Nash KM, Shah ZA (2015) Current perspectives on the beneficial role of *Ginkgo biloba* in neurological and cerebrovascular disorders. Integr Med Res 10:1–9

Peng M, Shahzad R, Gul A, Subthain H, Shen SQ, Lei L, Zheng ZG, Zhou JJ, Lu DD, Wang SC, Nishawy E, Liu XQ, Tohge T, Fernie AR, Luo J (2017) Differentially evolved glucosyltransferases determine natural variation of rice flavone accumulation and UV-tolerance. Nat Commun 8:1–12

Pertea M, Kim D, Pertea GM, Leek JT, Salzberg SL (2016) Transcript-level expression analysis of RNA-seq experiments with HISAT, StringTie and Ballgown. Nat Protoc 11:1650–1667

Phillips GC, Garda M (2019) Plant tissue culture media and practices: an overview. In Vitro Cell Dev-Pl 55:242–257

Phongtongpasuk S, Piemthongkham P (2014) Shikimic acid production from *Ginkgo biloba* via callus culture. Adv Mat Res 931–932:1524–1528

Popova EV, Lee EJ, Wu CH, Hahn EJ, Paek KY (2009) A simple method for cryopreservation of *Ginkgo biloba* callus. Plant Cell Tiss Org 97:337–343

Radia A, Jocelyne TG (2003) Root formation from transgenic calli of *Ginkgo biloba*. Tree Physiol 23:713–718

Santiago LJM, Louro RP, De Oliveira DE (2000) Compartmentation of phenolic compounds and phenylalanine ammonia-lyase in leaves of *Phyllanthus tenellus* Roxb. and their induction by copper sulphate. Ann Bot-London 86:1023–1032

Shi R, Shuford CM, Wang JP, Sun YH, Yang Z, Chen HC, Tunlaya-Anukit S, Li Q, Liu J, Muddiman DC, Sederoff RR, Chiang VL (2013) Regulation of phenylalanine ammonia-lyase (PAL) gene family in wood forming tissue of *Populus trichocarpa*. Planta 238:487–497

Singh CR (2018) Review on problems and its remedy in plant tissue culture. Asian J Biol Life Sci 11:165–172

Smith CA, O'Maille G, Want EJ, Qin C, Trauger SA, Brandon TR, Custodio DE, Abagyan R, Siuzdak G (2005) METLIN: a metabolite mass spectral database. Ther Drug Monit 27:747–751

Su XJ, Shen GA, Di SK, Dixon RA, Pang YZ (2017) Characterization of *UGT716A1* as a multi-substrate UDP: flavonoid glucosyltransferase gene in *Ginkgo biloba*. Front Plant Sci 8:2085

Suekawa M, Fujikawa Y, Esaka M (2019) Exogenous proline has favorable effects on growth and browning suppression in rice but not in tobacco. Plant Physiol Bioch 142:1–7

Tang W, Newton RJ, Outhavong V (2004) Exogenously added polyamines recover browning tissues into normal callus cultures and improve plant regeneration in pine. Physiol Plantarum 122:386–395

Toivonen PM, Brummell DA (2008) Biochemical bases of appearance and texture changes in fresh-cut fruit and vegetables. Postharvest Biol Tec 48:1–14

Tsugawa H, Cajka T, Kind T, Ma Y, Higgins B, Ikeda K, Kanazawa M, VanderGheynst J, Fiehn O, Arita M (2015) MS-DIAL: data-independent MS/MS deconvolution for comprehensive metabolome analysis. Nat Methods 12:523–526

Wang L, Cui JW, Jin B, Zhao JG, Xu HM, Lu ZG, Li WX, Li XX, Li LL, Liang EY, Rao XL, Wang SF, Fu CX, Cao FL, Dixon RA, Lin JX (2020) Multifeature analyses of vascular cambial cells reveal longevity mechanisms in old *Ginkgo biloba* trees. Proc Natl Acad Sci USA 117:2201–2210

Wen W, Alseekh S, Fernie AR (2020) Conservation and diversification of flavonoid metabolism in the plant kingdom. Curr Opin Plant Biol 55:100–108

Wilson AE, Tian L (2019) Phylogenomic analysis of UDP-dependent glycosyltransferases provides insights into the evolutionary landscape of glycosylation in plant metabolism. Plant J 100:1273–1288

Xie C, Mao XZ, Huang JJ, Ding Y, Wu JM, Dong S, Kong L, Gao G, Li CY, Wei LP (2011) KOBAS 2.0: a web server for annotation and identification of enriched pathways and diseases. Nucleic Acids Res 39:W316–W322

Xu CJ, Zeng BY, Huang JM, Huang W, Liu YM (2015a) Genome-wide transcriptome and expression profile analysis of *Phalaenopsis* during explant browning. PLoS ONE 10:e0123356

Xu WJ, Dubos C, Lepiniec L (2015b) Transcriptional control of flavonoid biosynthesis by MYB-bHLH-WDR complexes. Trends Plant Sci 20:176–185

Xu NT, Liu S, Lu ZG, Pang SY, Wang L, Wang L, Li WX (2020) Gene expression profiles and flavonoid accumulation during salt stress in *Ginkgo biloba* seedlings. Plants 9:1162

Yang B, Liu HL, Yang JL, Gupta VK, Jiang YM (2018) New insights on bioactivities and biosynthesis of flavonoid glycosides. Trends Food Sci Tech 79:116–124

Yang XM, Zhou TT, Su XY, Wang GB, Zhang XH, Guo QR, Cao FL (2021a) Structural characterization and comparative analysis of the chloroplast genome of *Ginkgo biloba* and other gymnosperms. J for Res 32:765–778

Yang XM, Zhou TT, Wang MK, Li TT, Wang GB, Fu FF, Cao FL (2021b) Systematic investigation and expression profiles of the GbR2R3-MYB transcription factor family in ginkgo (*Ginkgo biloba* L.). Int J Biol Macromol 172:250–262

Yonekura-Sakakibara K, Hanada K (2011) An evolutionary view of functional diversity in family 1 glycosyltransferases. Plant J 66:182–193

Yonekura-Sakakibara K, Higashi Y, Nakabayashi R (2019) The origin and evolution of plant flavonoid metabolism. Front Plant Sci 10:943

Young MD, Wakefield MJ, Smyth GK, Oshlack A (2010) Gene ontology analysis for RNA-seq: accounting for selection bias. Genome Biol 11:R14

Zhang WW, Xu F, Cheng SY, Liao YL (2018) Characterization and functional analysis of a MYB gene (*GbMYBFL*) related to flavonoid accumulation in *Ginkgo biloba*. Genes Genom 40:49–61

Zhang K, Su JJ, Xu M, Zhou ZH, Zhu XY, Ma X, Hou JJ, Tan LB, Zhu ZF, Cai HW, Liu FX, Sun HY, Gu P, Li C, Liang YT, Zhao WS, Sun CQ, Fu YC (2020) A common wild rice-derived *BOC1*

allele reduces callus browning in indica rice transformation. Nat Commun 11:443

Zhang WW, Liu CQ, Zhao J, Ma TY, He ZD, Huang MG, Wang YS (2021) Modification of structure and functionalities of ginkgo seed proteins by pH-shifting treatment. Food Chem 358:129862

Zhao YP, Fan GY, Yin PP, Sun S, Li N, Hong XN, Hu G, Zhang H, Zhang FM, Han JD, Hao YJ, Xu QW, Yang XW, Xia WJ, Chen WB, Lin HY, Zhang R, Chen J, Zheng XM, Lee SM, Lee J, Uehara K, Wang J, Yang HM, Fu CX, Liu X, Xu X, Ge S (2019) Resequencing 545 ginkgo genomes across the world reveals the evolutionary history of the living fossil. Nat Commun 10:4201

Zhou ZY (2009) An overview of fossil Ginkgoales. Palaeoworld 18:1–22

Zhou TT, Yang XM, Fu FF, Wang GB, Cao FL (2020) Selection of suitable reference genes based on transcriptomic data in *Ginkgo biloba* under different experimental conditions. Forests 11:1217